Separation Science and Technology
Publication details, including instructions for authors and subscription information:
http://www.informaworld.com/smpp/title~content=t713708471

Simulation of Multicomponent Distillation Using a Nonequilibrium Stage Model

Gabriel Ovejero[a]; Rafael Van Grieken[a]; Lourdes Rodriguez[a]; Jose Luis Valverde[a]
[a] DEPARTMENTO INGENIERIA QUIMICA, FACULTAD DE CIENCIAS QUIMICAS UNIVERSIDAD COMPLUTENSE DE MADRID, MADRID, SPAIN

To cite this Article Ovejero, Gabriel , Van Grieken, Rafael , Rodriguez, Lourdes and Valverde, Jose Luis(1994) 'Simulation of Multicomponent Distillation Using a Nonequilibrium Stage Model', Separation Science and Technology, 29: 14, 1805 — 1821
To link to this Article: DOI: 10.1080/01496399408002174
URL: http://dx.doi.org/10.1080/01496399408002174

SEPARATION SCIENCE AND TECHNOLOGY, **29**(14), pp. 1805–1821, 1994

Simulation of Multicomponent Distillation Using a Nonequilibrium Stage Model

GABRIEL OVEJERO, RAFAEL VAN GRIEKEN,
LOURDES RODRIGUEZ, and JOSE LUIS VALVERDE
DEPARTAMENTO INGENIERIA QUIMICA
FACULTAD DE CIENCIAS QUIMICAS
UNIVERSIDAD COMPLUTENSE DE MADRID
28040-MADRID, SPAIN

ABSTRACT

A nonequilibrium stage model is used to predict composition profiles for binary and multicomponent distillation in a column of spheres and cylinders with a known interfacial area. The profiles generated by the model are compared with experimental data for the binary systems methanol–isopropanol, methanol–water, and isopropanol–water, and for the ternary systems methanol–isopropanol–water and acetone–*n*-hexane–cyclohexane. The model predicts with a high accuracy the experimental data with an average deviation lower than 1 mol%.

Key Words. Distillation; Nonequilibrium model; Interaction effects; Nonideal systems

INTRODUCTION

Simulation of multicomponent separation processes such as distillation and absorption is a powerful tool for the modern chemical engineer. At present these simulations are based on the equilibrium-stage model (1–4). However, industrial columns rarely operate at equilibrium conditions. The usual method to take into account deviations from the equilibrium in multistage towers is to incorporate a stage efficiency into the equilibrium relations. While many different models of stage efficiency have been pro-

posed for binary systems (1, 5–7), the extension of these models to multicomponent systems involves several complications, mainly due to possible coupling between the individual concentration gradients.

During the last few years, different researchers have been working on the development of nonequilibrium stage models which avoid the use of ambiguous stage efficiencies for multicomponent separation processes (8–13). The nonequilibrium stage model used in this work was developed by Krishnamurthy and Taylor (8) for the simulation of countercurrent multicomponent separation processes.

In the present work this nonequilibrium model has been tested using data obtained in a wetted-wall column for nonideal systems: three binary and two ternary mixtures. A new solving method using the Marquardt algorithm has been proposed (14).

The Nonequilibrium Model

The model consists of material and energy balances for each phase, models for interphase mass and energy transfer, and equilibrium equations to relate the interface compositions. The equations representing the jth stage or jth section of packing, whose schematic representation is shown in Fig. 1, are as follows.

The Conservation Equations

It is possible to establish c component material balances for each phase:

$$M_{ij}^{V} \equiv (1 + r_j^{V})v_{ij} - v_{ij-1} - f_{ij}^{V} + \mathcal{N}_{ij}^{V} = 0 \tag{1}$$

$$M_{ij}^{L} \equiv (1 + r_j^{L})l_{ij} - l_{ij+1} - f_{ij}^{L} - \mathcal{N}_{ij}^{L} = 0 \tag{2}$$

where $\mathcal{N}_{ij}^{V}$ and $\mathcal{N}_{ij}^{L}$ represents the interphase molar flows of species i from the vapor and to the liquid, respectively, and

$$r_j^{V} = S_j^{V}/V_j; \qquad r_j^{L} = S_j^{L}/L_j \tag{3}$$

are the ratios of side stream to interstage flow rates.

The energy balances for each phase are

$$E_j^{V} \equiv (1 + r_j^{V})V_jH_j^{V} + Q_j^{V} - V_{j-1}H_{j-1}^{V} - F_j^{V}H_j^{VF} + \mathcal{E}_j^{V} = 0 \tag{4}$$

$$E_j^{L} \equiv (1 + r_j^{L})L_jH_j^{L} + Q_j^{L} - L_{j+1}H_{j+1}^{L} - F_j^{L}H_j^{LF} - \mathcal{E}_j^{L} = 0 \tag{5}$$

where $\mathcal{E}_j^{V}$ and $\mathcal{E}_j^{L}$ represent the interphase energy flow rates.

The balances around the interphase lead to

$$M_{ij}^{I} \equiv \mathcal{N}_{ij}^{V} - \mathcal{N}_{ij}^{L} = 0 \tag{6}$$

$$E_j^{I} \equiv \mathcal{E}_j^{V} - \mathcal{E}_j^{L} = 0 \tag{7}$$

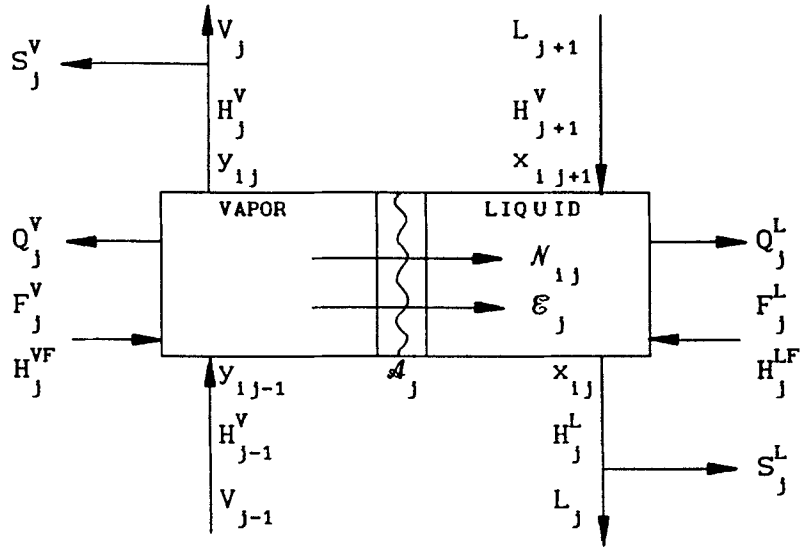

FIG. 1 Schematic representation of a nonequilibrium stage.

From Eq. (6) there is only a set of c independent molar transfer flows, $\mathcal{N}_{ij}$ ($= \mathcal{N}_{ij}^{V} = \mathcal{N}_{ij}^{L}$), and therefore we can define the following balance equations:

$$R_{ij}^{V} \equiv \mathcal{N}_{ij} - \mathcal{N}_{ij}^{V} = 0 \tag{8}$$

$$R_{ij}^{L} \equiv \mathcal{N}_{ij} - \mathcal{N}_{ij}^{L} = 0 \tag{9}$$

Mass Transfer Rate Equations

The precise form of the mass transfer rate equations depends on the model used to represent the vapor-phase transport processes. Using the equations based on film model steady-state one-dimensional diffusion, there are several methods of calculating the fluxes. These methods may be grouped in three categories.

1. Methods Based on the Use of an Effective Mass Transfer Coefficient, k_{ieff}^{V}. These methods neglect interactions between species, and the mass transfer rates are given by

$$\mathcal{N}_i^{V} = k_{ieff}^{V} \mathcal{A} \Phi_{ieff}^{V} (\bar{y}_i^{V} - y_i^{I}) + \bar{y}_i^{V} \mathcal{N}_t^{V}, \qquad i = 1, 2, 3, \ldots, c-1 \tag{10}$$

where k_{ieff}^{V} depends on the effective diffusivities. Φ_{ieff}^{V} is a correction factor

due to high mass flux and is calculated as follows (15):

$$\Phi^{V}_{ieff} = \frac{\phi^{V}_{ieff}}{\exp \phi^{V}_{ieff} - 1} \tag{11}$$

$$\phi^{V}_{ieff} = k^{V}_{ieff}\mathcal{A}/\mathcal{N}_t \tag{12}$$

There are several ways to estimate the effective mass transfer coefficient. Wilke's (16) formula for the effective diffusion coefficient, modified here in order to obtain effective mass transfer coefficients, is the one most used in the literature (8):

$$k^{V}_{ieff} = \frac{1 - y'_i}{\sum_{k=1}^{c} (y'_k/k^{V}_{ik})} \tag{13}$$

where $y'_i = 0.5(\bar{y}^{V}_i + y^{I}_i)$.

The lack of interaction effects in the model is the main disadvantage of these methods.

2. Implicit Interactive Methods. Two method fall into this category: that based on the exact solution of the Maxwell–Stefan equations (17) and that based on the solution of linearized equations (18–20). Both methods lead to the following equation:

$$(\mathcal{N}^{V}) = [k^{V}]\mathcal{A}(\bar{y} - y^{I}) + \mathcal{N}^{V}_t(\bar{y}) \tag{14}$$

where $(\mathcal{N}^{V})$ is the column matrix with $c - 1$ elements of mass transfer rates through the vapor phase

$(\bar{y} - y^{I})$ is the column matrix with $c - 1$ concentration differences between the bulk vapor phase and the interface for each component

$[k^{V}]$ is the square matrix with $(c - 1) \times (c - 1)$ multicomponent mass transfer coefficients and is calculated (17):

$$[k^{V}]\mathcal{A} = [B^{V}]^{-1}\mathcal{A}[\Lambda^{V}]\{\exp[\Lambda^{V}] - [I]\}^{-1} \tag{15}$$

The elements of $[B^{V}]$ and $[\Lambda^{V}]$ may be defined using a general matrix [M] whose elements are functions of binary mass transfer coefficients k^{V}_{ij}:

$$M_{ii} = \frac{m_i}{k_{ic}\mathcal{A}} + \sum_{\substack{k=1 \\ k \neq i}}^{c} \frac{m_k}{k_{ik}\mathcal{A}}; \qquad i = 1, 2, \ldots, c - 1 \tag{16}$$

$$M_{ik} = -m_i\left[\frac{1}{k_{ik}\mathcal{A}} - \frac{1}{k_{ic}\mathcal{A}}\right]; \qquad i \neq k = 1, 2, \ldots, c - 1 \tag{17}$$

where the k_{ik} are the mass transfer coefficients of the binary i–k pair. These coefficients must be estimated from a suitable correlation of experimental data, such as the one we propose further on. In the method of Krishna and Standart (17), $[B^V]/\mathscr{A} = [M]$ with $m_i = \bar{y}_i$ and $[\Lambda^V] = [M]$ with $m_i = \mathscr{N}_i^V$.

3. Explicit Interactive Method. In these methods the rate equations take the form

$$(\mathscr{N}^V) = [K^V]\Phi^V\mathscr{A}(\bar{y} - y^I) \tag{18}$$

where $[K^V]$ is the square matrix of total mass transfer coefficients and Φ^V is a flux correction factor.

Energy Transfer Rate Equations

The film model of simultaneous heat and mass transfer in multicomponent systems leads to the following expression for the energy transfer rate through the vapor film (15, 17):

$$\mathscr{E}^V = h^V\mathscr{A}\frac{E^V}{\exp E^V - 1}(\bar{T}^V - T^I) + \sum_{i=1}^{c}\bar{H}_i^V\mathscr{N}_i \tag{19}$$

where E^V is defined by

$$E^V = \frac{\sum_{i=1}^{c}\mathscr{N}_i Cp_i^V}{h^V\mathscr{A}} \tag{20}$$

and h^V is the vapor phase heat transfer coefficient, estimated from the appropriate correlation (see below).

For the liquid phase, a similar relation to Eq. (17) can be written for low transfer flux:

$$\mathscr{E}^L = h^L\mathscr{A}(T^I - \bar{T}^L) + \sum_{i=1}^{c}\bar{H}_i^L\mathscr{N}_i \tag{21}$$

where h^L is the heat transfer coefficient for the liquid phase.

Interface Equations

Assuming a singular surface offering no resistance to transport, where equilibrium is attained, the following equations relate the mole fractions on each side of the interface:

$$Q_{ij}^I = K_{ij}x_{ij}^I - y_{ij}^I = 0 \tag{22}$$

$$\Sigma_j^V = \sum_{i=1}^{c} y_{ij}^I - 1 = 0, \qquad \Sigma_j^L = \sum_{i=1}^{c} x_{ij}^I - 1 = 0 \tag{23}$$

Thermodynamic and Transport Properties Evaluation

To solve the equations of the model described above, evaluation of the following thermodynamic properties is need: K values at the temperature and composition of the interface, enthalpies of the vapor and liquid streams entering and leaving every stage, and partial molar enthalpies of the bulk vapor and liquid phase. All these thermodynamic properties have been calculated by using the methods proposed by Prausnitz et al. (21).

Solving the equations system also requires the evaluation of the transport coefficients (binary mass transfer and heat transfer coefficients) which involves the calculation of several other physical and transport properties: binary diffusion coefficients, viscosity, density, heat capacity, and thermal conductivity. The binary mass transfer coefficients have been calculated from the experimental correlation proposed in a previous work for the same type of contact device (22):

$$\frac{k_{ik}^{V} RT^{V}}{V_R} = 0.195\left(\frac{V_R \rho_{ik}^{V}}{a_s \mu_{ik}^{V}}\right)^{-1/3}\left(\frac{\mu_{ik}^{V}}{\rho_{ik}^{V} D_{ik}^{V}}\right)^{-1/2} \tag{24}$$

$$\frac{k_{ik}^{L}}{a_s D_{ik}^{L}} = 2.79\left(\frac{L_m \rho_{ik}^{L}}{\mu_{ik}^{L}}\right)^{2/3}\left(\frac{\mu_{ik}^{L}}{\rho_{ik}^{L} D_{ik}^{L}}\right)^{1/3}\left(\frac{g(\rho_{ik}^{L})^2}{(\mu_{ik}^{L})^2 a_s^3}\right)^{0.38}\left(\frac{(\mu_{ik}^{L})^2 a_s}{\rho_{ik}^{L}\sigma_{ik}^{L}}\right)^{0.42} \tag{25}$$

The properties have been calculated separately on each stage by the predictive methods recommended by Reid et al. (23).

EXPERIMENTAL

The data were obtained by using an experimental device which has been previously described elsewhere (24). The experiments were carried at total reflux and steady-state conditions that considerably reduce the number of equations in the model, since $x_{ij+1} = y_{ij}$ and $l_{ij+1} = v_{ij}$ at any height of the column. Moreover, in these types of experiments the maximum separation is attained for a given number of stages and no material is lost from the column.

Sequence data collection from different parts of the column was repeated twice consecutively, with about 15 minute between reading or sampling at the same height of the column.

The binary systems used were methanol–water, isopropanol–water, and methanol–isopropanol, and the ternary systems used were methanol–isopropanol–water and acetone–*n*-hexane–cyclohexane.

THE SIMULATIONS

The experiments were simulated by dividing the column into six sections, each of which was treated as though it were a nonequilibrium stage.

Moreover, the distillation column was equipped with a partial reboiler and a total condenser.

The partial reboiler was modeled as an equilibrium stage with $(2c + 1)$ variables: c component liquid flow rate, l_{ij}; c component vapor flow rate, v_{ij}; and the temperature $T_j^{\mathrm{L}} = T_j^{\mathrm{V}} = T_j^{\mathrm{I}}$. The $(2c + 1)$ equations that model this stage included the c component material balance, c equilibrium relationships, and the energy balance.

The total condenser may be described by a set of $(2c + 1)$ equations: c component material balance, an energy balance, $(c - 1)$ equations which consider the equality between the mole fractions in the product and reflux streams, and an equation specifying the temperature of the product stream.

Each one of the nonequilibrium stages is described through $(6c + 5)$ equations and independent variables, as mentioned before. A reduction in this large number of equations and independent variables can be obtained by eliminating certain linearly dependent equations. So, considering that there is only one set of c strictly independent mass transfer rates, $\mathcal{N}_{ij}$ $(= \mathcal{N}_{ij}^{\mathrm{V}} = \mathcal{N}_{ij}^{\mathrm{L}})$, and combining the energy balance in the interface (7) with the energy transfer rate equations (19) and (20), the final number of equations and independent variables to be considered is $(5c + 3)$, expressed in vectorial form as follows.

Independent variables:

$$\mathbf{x}_j \equiv (v_{1j}, v_{2j}, \ldots, v_{cj}, l_{1j}, l_{2j}, \ldots, l_{cj}, T_j^{\mathrm{V}}, T_j^{\mathrm{L}}, \mathcal{N}_{1j}, \mathcal{N}_{2j}, \ldots, \mathcal{N}_{cj}, y_{1j}^{\mathrm{I}}, y_{2j}^{\mathrm{I}}, \ldots, y_{cj}^{\mathrm{I}}, x_{1j}^{\mathrm{I}}, x_{2j}^{\mathrm{I}}, \ldots, x_{cj}^{\mathrm{I}}, T_j^{\mathrm{I}}) \quad (26)$$

Independent equations:

$$\mathbf{F}_j \equiv (M_{1j}^{\mathrm{V}}, M_{2j}^{\mathrm{V}}, \ldots, M_{cj}^{\mathrm{V}}, M_{1j}^{\mathrm{L}}, M_{2j}^{\mathrm{L}}, \ldots, M_{cj}^{\mathrm{L}}, R_{1j}^{\mathrm{V}}, R_{2j}^{\mathrm{V}}, \ldots, R_{c-1j}^{\mathrm{V}}, R_{1j}^{\mathrm{L}}, R_{2j}^{\mathrm{L}}, \ldots, R_{c-1j}^{\mathrm{L}}, E_j^{\mathrm{V}}, E_j^{\mathrm{L}}, E_j^{\mathrm{I}}, Q_{1j}^{\mathrm{I}}, Q_{2j}^{\mathrm{I}}, \ldots, Q_{cj}^{\mathrm{I}}, \Sigma_j^{\mathrm{V}}, \Sigma_j^{\mathrm{L}}) \quad (27)$$

The experiments were carried out at total reflux, for which $v_{ij} = l_{ij+1}$, and therefore the set of component vapor flows, v_{ij}, or the component liquid flows, l_{ij}, can be removed from the set of variables representing the jth nonequilibrium stage.

The sequence of the six nonequilibrium stages will be described by a set of $6(4c + 3) = (24c + 18)$ variables and equations, and the distillation column will be represented by $(2c + 1) + (24c + 18) + (2c + 1) = (28c + 20)$ variables related through the same number of equations.

A simple flow chart of the calculation algorithm used in the simulation of the distillation experiments could be expressed as shown in Chart 1.

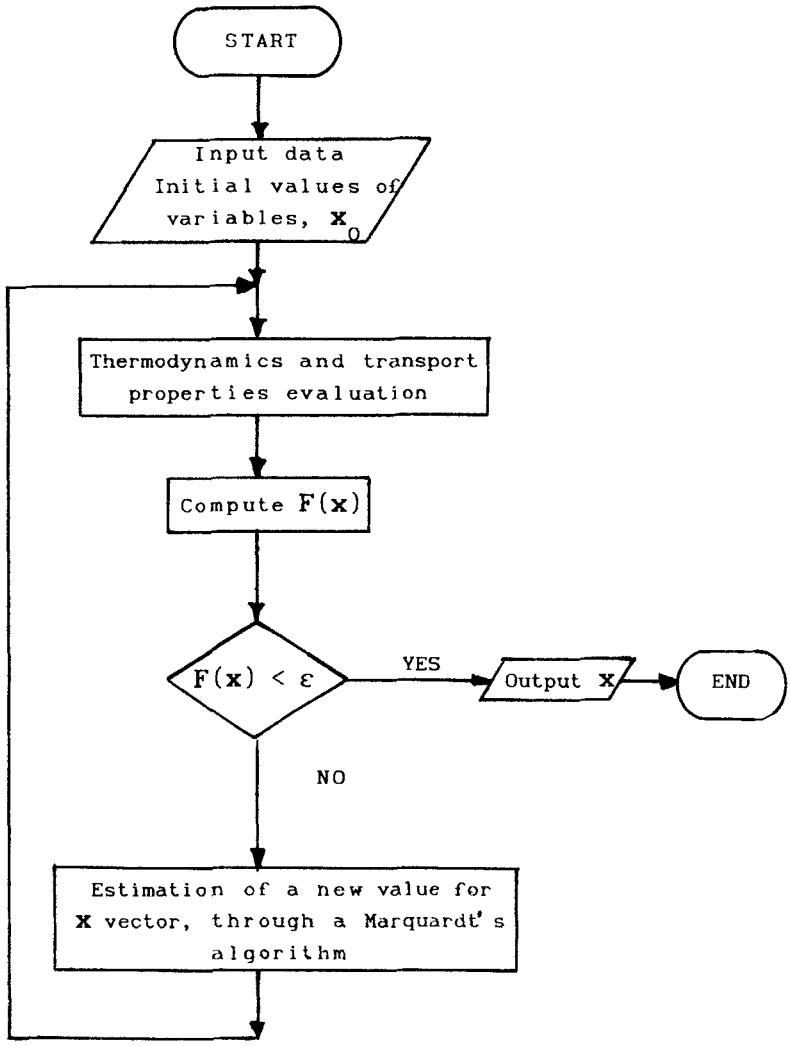

CHART I

RESULTS AND DISCUSSION

In our simulations the composition measured at the column bottom was used to initiate calculation of the profiles along the column. Figures 2(a–c) show a comparison between the experimental data and the profiles predicted by the model for some runs carried out with the three binary sys-

tems methanol–isopropanol, methanol–water, and isopropanol–water. As can be seen, the discrepancies are extremely small, with an average absolute deviation of much less than 1% (Fig. 3).

A much better test of the model is provided by comparison between its predictions and the measured profiles in multicomponent systems. Predicted and measured composition profiles for the systems methanol, isopropanol, and water (Figs. 4, 5, and 6) and acetone, *n*-hexane, and cyclohexane (Figs. 7, 8, and 9) show excellent agreement, with average and maximum error values very low.

To determine the influence of the interaction effects among the different components forming the ternary system, a new simulation has been made by replacing Eq. (12) by Eq. (8), described above, for the acetone–*n*-hexane–cyclohexane system. Figures 7 and 8 show comparisons among the experimental values, the predicted composition profiles by the interactive model (Eq. 12), and the predicted composition profiles by the effective diffusivity model (Eq. 8). The average deviation in prediction of the experimental values is around 6%.

Finally, Figs. 7 and 8 also show the results obtained for the acetone–*n*-hexane–cyclohexane system using an equilibrium stage model to estimate the composition profiles. A clear difference between the experimental values and the estimated composition profiles can be observed with an average error above 15%.

The agreement between the experimental results and the values predicted by the nonequilibrium model with interaction effects in all the simulations carried out with different systems is almost complete, showing the excellent possibilities of the model, useful when dealing with nonideal systems. Among the different information sources needed by this predictive model, the correlations of mass transfer coefficients used in this work lead to adequate estimation of the molar fluxes in every stage.

The influence of the interaction effects is easily deduced from a comparison of the predicted profiles by the nonequilibrium model with interaction effects and without them; the latter is based on the effective diffusivity method. These interaction effects become important in the systems used in these work in which the binary pair diffusivities differ widely. As can be observed from Figs. 7 and 8, ignoring the interaction effects leads to poorer predictive results.

The equilibrium stage model has been used to estimate the importance of mass transfer resistance between phases. The number of equilibrium stages needed to reach the experimental composition of the column top was determined for each experiment, starting from the experimental composition of the column bottom. The number of equilibrium stages, and therefore the height equivalent to a theoretical plate (HETP), varies with

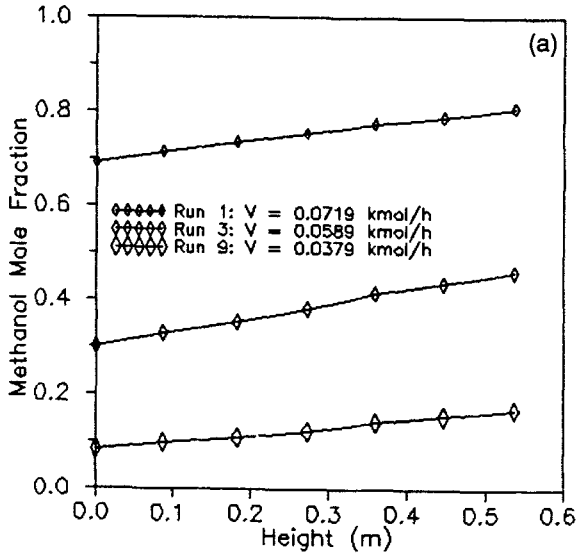

FIG. 2(a) Comparison of experimental and predicted composition profiles for the binary system methanol and isopropanol.

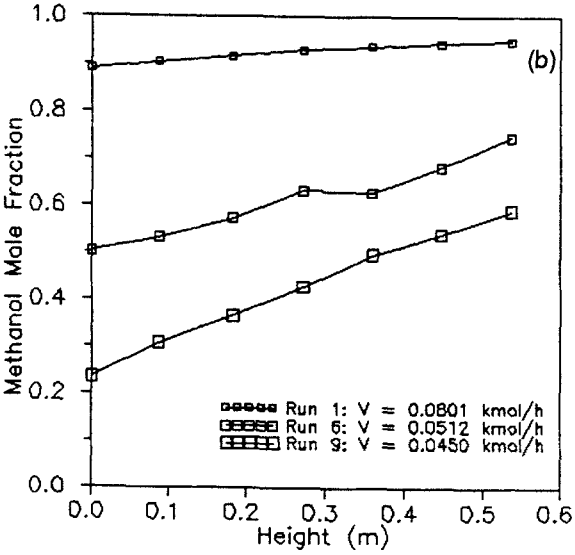

FIG. 2(b) Comparison of experimental and predicted composition profiles for the binary system methanol and water.

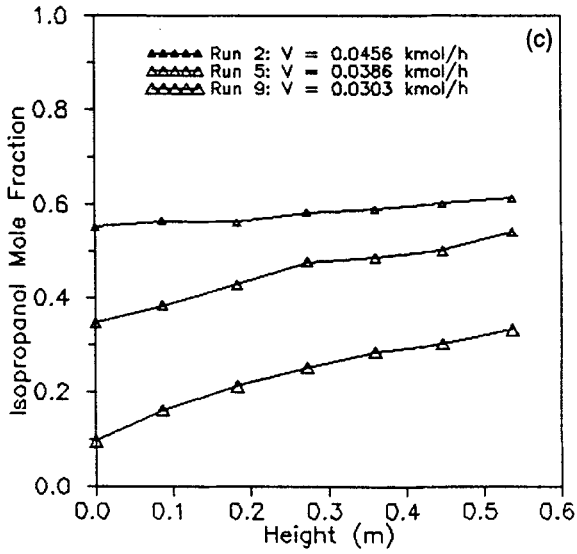

FIG. 2(c) Comparison of experimental and predicted composition profiles for the binary system isopropanol and water.

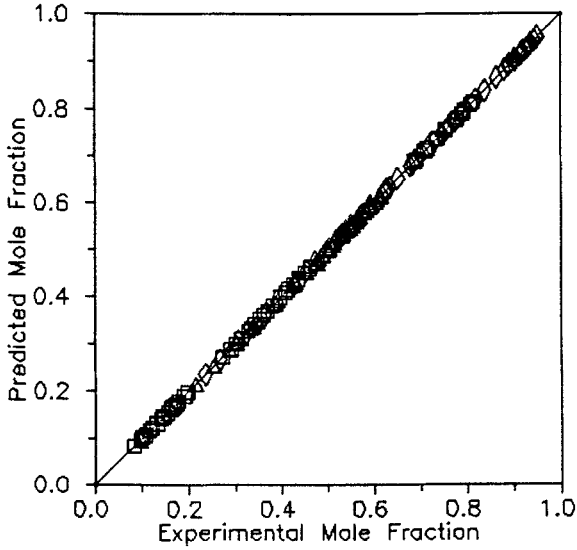

FIG. 3 Comparison of experimental and predicted mole fractions for the binary systems: methanol and isopropanol (◇), methanol and water (□) and isopropanol and water (△).

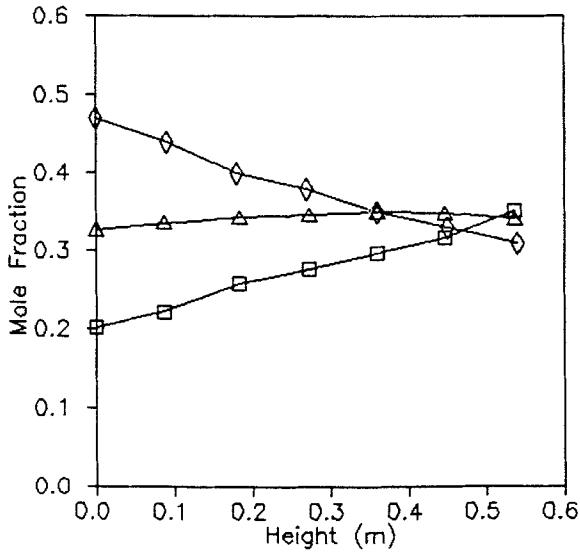

FIG. 4 Comparison of experimental and predicted composition profiles for the methanol (□), isopropanol (△), and water (◇) systems. Predicted profile: (——). Run 2: V = 0.0916 kmol/h.

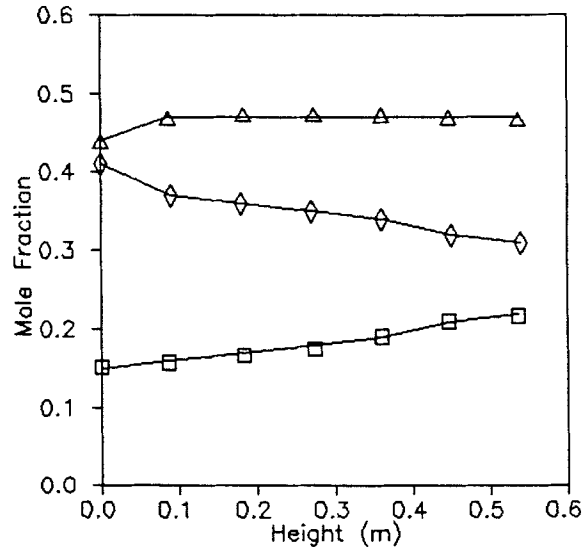

FIG. 5 Comparison of experimental and predicted composition profiles for the methanol (□), isopropanol (△), and water (◇) systems. Predicted profile (——). Run 8: V = 0.0600 kmol/h.

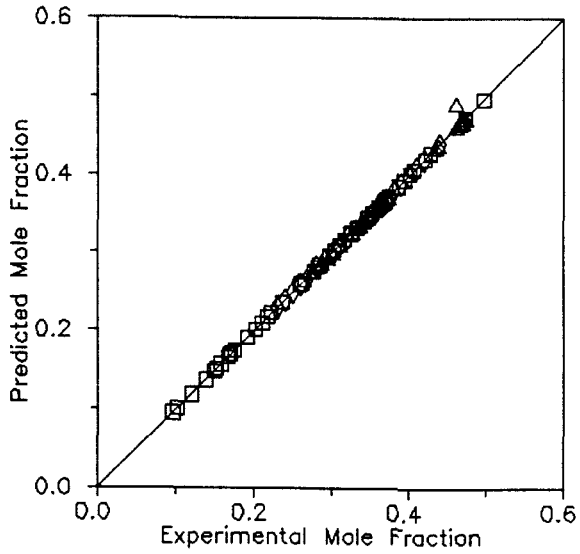

FIG. 6 Comparison of experimental and predicted mole fractions for methanol (□), isopropanol (△), and water (◇) systems.

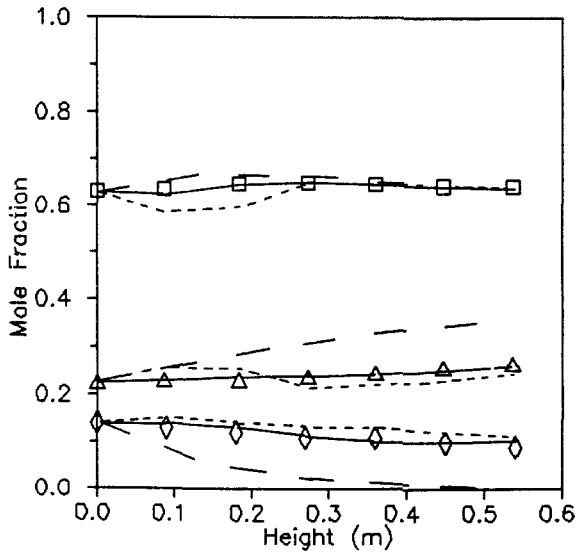

FIG. 7 Comparison of experimental and predicted composition profiles for the acetone (□), *n*-hexane (△) and cyclohexane (◇) systems. Predicted profile by nonequilibrium model with interactions (——). Predicted profile by nonequilibrium model with effective diffusivity (- - -). Predicted profile by the equilibrium stage model (– –). Run 1: V = 0.0273 kmol/h.

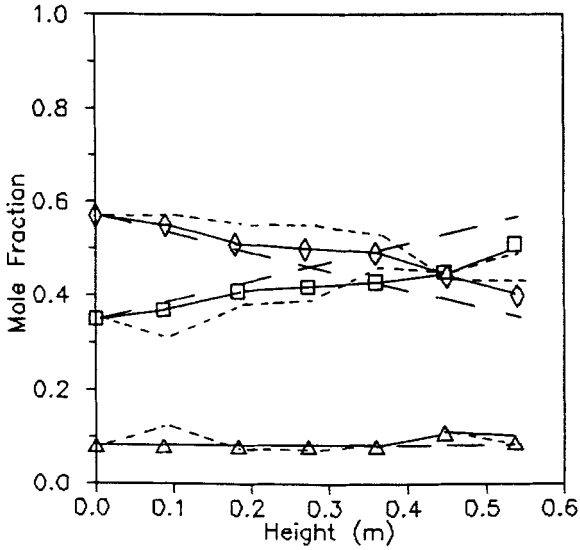

FIG. 8 Comparison of experimental and predicted composition profiles for the acetone (□), *n*-hexane (△), and cyclohexane (◇) systems. Predicted profile by nonequilibrium model with interactions (——). Predicted profile by nonequilibrium model with effective diffusivity (- - -). Predicted profile by the equilibrium stage model (– –). Run 7: V = 0.0425 kmol/h.

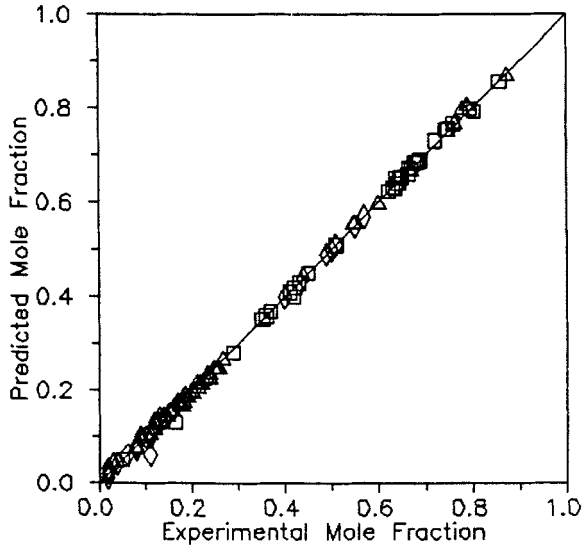

FIG. 9 Comparison of experimental and predicted mole fractions for acetone (□), *n*-hexane (△), and cyclohexane (◇) systems.

the composition of the column bottom without any relation between these variables.

SYMBOLS

$\mathcal{A}$	interfacial area (m^2)
a_s	specific interfacial area of packing (m^2/m^3)
[B]	matrix of inverse mass transfer coefficients ($m^2 \cdot s/kmol$)
D	diffusivity (m^2/s)
c	number of component
Cp	specific heat (J/kmol·K)
E	energy balance functions (J/s)
E	heat transfer rate factor
$\mathscr{E}$	total interphase energy transfer rate (J/s)
f	component feed rate (kmol/s)
F	total feed rate (kmol/s)
g	gravitational acceleration (m/s^2)
h	heat transfer coefficient ($J/s \cdot m^2 \cdot K$)
$\underline{H}$	enthalpy (J/kmol)
$\overline{H}$	partial molar enthalpy (J/kmol)
[I]	identity matrix
k	individual mass transfer coefficient ($kmol/m^2 \cdot s$)
[K]	square matrix of total mass transfer coefficients
K_{ij}	equilibrium ratio
l	component liquid flow (kmol/s)
L	total liquid flow (kmol/s)
L_m	liquid flow rate [m^3/s (m perimeter)]
M	mass balance functions (kmol/s)
[M]	general matrix defined by Eqs. (14) and (15)
m	element of the matrix [M]
$\mathcal{N}$	total interphase mass transfer ratio (kmol/s)
$Q_{ij}^{\mathbf{I}}$	interphase equilibrium function
Q	heat removal (J/s)
r	ratio of side stream to interstage flow rate
S	total side stream flow (kmol/s)
T	temperature (K)
v	component vapor flow (kmol/s)
V	total vapor flow (kmol/s)
V_R	liquid–gas relative velocity (m/s)
x	liquid-phase composition (mole fraction)
y	vapor-phase composition (mole fraction)

Greek Letters

Φ	high flux correction factor
ϕ	rate factor
$[\Lambda]$	rate factor matrix
Σ	summatory functions
ρ	density (kg/m^3)
μ	viscosity ($kg/m \cdot s$)
σ	surface tension (kg/s^2)

Subscripts

eff	effective value (of property)
i, k	component number
j	stage number
t	total (of property)

Superscripts

I	interface
L	liquid bulk
LF	liquid feed
V	vapor bulk
VF	vapor feed
—	average bulk value

Matrices

( )	column matrix
[ ]	square matrix

REFERENCES

1. C. D. Holland, *Fundamentals and Modeling of Separation Processes*, Prentice-Hall, Englewood Cliffs, New Jersey, 1975.
2. C. D. Holland, *Fundamentals of Multicomponent Distillation*, McGraw-Hill, New York, 1981.
3. E. J. Henley and J. D. Seader, *Equilibrium Stage Separation Operations in Chemical Engineering*, Wiley, New York, 1981.
4. C. J. King, *Separation Processes*, 2nd ed., McGraw-Hill, New York, 1980.
5. E. V. Murphee, "Rectifying Column Calculations with Particular References to *n*-Component Mixtures," *Ind. Eng. Chem.*, *17*, 747–750 (1925).
6. H. Hausen, "A Definition of Exchange Efficiency of Rectifying Plates for Binary and Ternary Mixtures," *Chem.-Ing.-Tech.*, *25*, 595–597 (1953).
7. G. L. Standart, "Distillation. V. Generalized Definition of a Theoretical Plate or Stage of Contacting Equipment," *Chem. Eng. Sci.*, *20*, 611–622 (1965).

8. R. Krishnamurthy and R. Taylor, "A Nonequilibrium Stage Model of Multicomponent Separation Processes. I. Model Description and Method of Solution," *AIChE J.*, *31*, 449–456 (1985).
9. R. Krishnamurthy and R. Taylor, "A Nonequilibrium Stage Model of Multicomponent Separation Processes. II. Comparison with Experiments," *Ibid.*, *31*, 456–465 (1985).
10. R. Krishnamurthy and R. Taylor, "A Nonequilibrium Stage Model of Multicomponent Separation Processes. III. The Influence of Unequal Efficiencies in Process Design Problems," *Ibid.*, *31*, 1973–1985 (1985).
11. R. Krishnamurthy and R. Taylor, "Simulation of Packed Distillation and Absorption Columns," *Ind. Eng. Chem., Process Des. Dev.*, *24*, 513–524 (1985).
12. R. Taylor, M. F. Powers, A. Arehole, and M. Lao, "The Development of Nonequilibrium Model for Component Simulation of Multicomponent Distillation and Absorption Operations," *Proc. Chem. Symp. Distillation Absorption, Brighton*, p. B321 (1987).
13. M. F. Powers, D. J. Wickery, A. Arehole, and R. Taylor, "A Nonequilibrium Stage Model of Multicomponent Separation Processes. V. Computational Methods for Solving the Model Equations," *Comput. Chem. Eng.*, *12*, 1229–1241 (1988).
14. D. W. Marquardt, "An Algorithm for Least-Squares Stimulation of Nonlinear Parameters," *J. Soc. Ind. Appl. Math.*, *11*, 471–481 (1983).
15. R. B. Bird, W. E. Stewart, and E. N. Lightfoot, *Transport Phenomena*, Wiley, New York, 1980, p. 656.
16. C. R. Wilke, "Diffusional Properties of Multicomponent Gases," *Chem. Eng. Prog.*, *46*, 95–104 (1950).
17. R. Krishna and G. L. Standart, "Mass and Energy Transfer in Multicomponent Systems," *Chem. Eng. Commun.*, *3*, 201–275 (1979).
18. H. L. Toor, "Solution of the Linearized Equations of Multicomponent Mass Transfer. I," *AIChE J.*, *10*, 448–455 (1964).
19. H. L. Toor, "Solution of the Linearized Equations of Multicomponent Mass Transfer. II. Matrix Methods," *Ibid.*, *10*, 460–465 (1964).
20. W. E. Stewart and R. Prober, "Matrix Calculation of Multicomponent Mass Transfer in Isothermal Systems," *Ind. Eng. Chem., Fundam.*, *3*, 224–235 (1964).
21. J. M. Prausnitz, R. F. Anderson, E. A. Grens, C. A. Eckert, R. Hsieh, and J. P. O'Connell, *Computer Calculations for Multicomponent Vapor–Liquid and Liquid–Liquid Equilibria*, Prentice-Hall, Englewood Cliffs, New Jersey, 1980.
22. E. Costa, G. Ovejero, M. A. Uguina, and C. Lopez, "Mass Transfer in Liquids. Determination of Effective Specific Interfacial Areas for Packing," *Int. Chem. Eng.*, *32*, 292–301 (1992).
23. R. C. Reid, J. M. Prausnitz, and B. E. Poling, *The Properties of Gases and Liquids*, 4th ed., McGraw-Hill, New York, 1987.
24. G. Ovejero, R. Van Grieken, L. Rodriguez, and J. L. Valverde, "The Use of Gas Absorption Correlations for Mass Transfer Coefficients in Distillation Processes," *Int. J. Heat Mass Transfer*, *35*, 2963–2968 (1992).

Received by editor July 2, 1992
Revised November 22, 1993